J Infrared Milli Terahz Waves (2016) 37:881–893
DOI 10.1007/s10762-016-0279-4

Advances in Front-end Enabling Technologies for Thermal Infrared '*THz Torch*' Wireless Communications

Fangjing Hu [1,2] · **Stepan Lucyszyn** [1,2]

Received: 12 October 2015 / Accepted: 20 April 2016 /
Published online: 2 May 2016

Abstract The thermal (emitted) infrared frequency bands (typically 20–40 and 60–100 THz) are best known for remote sensing applications that include temperature measurement (e.g. non-contacting thermometers and thermography), night vision and surveillance (e.g. ubiquitous motion sensing and target acquisition). This unregulated part of the electromagnetic spectrum also offers commercial opportunities for the development of short-range secure communications. The '*THz Torch*' concept, which fundamentally exploits engineered blackbody radiation by partitioning thermally generated spectral radiance into pre-defined frequency channels, was recently demonstrated by the authors. The thermal radiation within each channel can be independently pulse-modulated, transmitted and detected, to create a robust form of short-range secure communications within the thermal infrared. In this paper, recent progress in the front-end enabling technologies associated with the *THz Torch* concept is reported. Fundamental limitations of this technology are discussed; possible engineering solutions for further improving the performance of such thermal-based wireless links are proposed and verified either experimentally or through numerical simulations. By exploring a raft of enabling technologies, significant enhancements to both data rate and transmission range can be expected. With good engineering solutions, the *THz Torch* concept can exploit nineteenth century physics with twentieth century multiplexing schemes for low-cost twenty-first century ubiquitous applications in security and defence.

Keywords Thermal infrared · *THz Torch* · Blackbody radiation · Wireless communications · Frequency division multiplexing · Frequency-hopping spread-spectrum

✉ Stepan Lucyszyn
s.lucyszyn@imperial.ac.uk

[1] Centre for Terahertz Science and Engineering, Imperial College London, London, UK

[2] Optical and Semiconductor Devices Group, Department of EEE, Imperial College London, Exhibition Road, London SW7 2AZ, UK

1 Introduction

Optical wireless communications have been widely used in modern communication systems. Transmission windows having relatively low atmospheric attenuation support the use of optical sources at specific wavelengths (e.g. 800 and 1550 nm and 10 μm) [1]. For 800-nm wireless links, low-cost light-emitting diodes (LEDs) and silicon-based photodiodes can be employed in the front-end of the transmitter and receiver, respectively. The main drawback for 800-nm technology relates to eye safety: it can potentially induce thermal damage to the retina [2]. The cornea is opaque to radiation at wavelengths above ~1.4 μm, greatly reducing ocular hazards. As a result, 1550-nm technologies are preferred from a safety perspective. However, detectors available for this range, which are usually made from germanium (Ge) or indium gallium arsenide (InGaAs), are more expensive when compared to silicon photodiodes. Moreover, both 800 nm and 1550 nm experience atmospheric absorption, scattering losses and scintillation effects [3], limiting their applications to indoor short-range communications.

By moving to the mid- or long-wavelength infrared (MWIR or LWIR) regions, improved link and increased transmission distance can be achieved, due to a lower susceptibility to atmospheric affects. For example, the 3–5- and 8–14-μm atmospheric transmission windows can be used, for their superior penetration of atmospheric obscurants such as fog, smoke and dust [4]. Within the MWIR (3–8 μm or 37–100 THz) and LWIR (8–15 μm or 20–37 THz), quantum cascade lasers (QCLs) [5–7] and 10 μm (or 30 THz) CO_2 lasers [3] are generally employed. However, these laser sources would be considered extravagant (non-ubiquitous) products for the domestic market, and only high-end users (e.g. scientific or military) can justify their high cost and, with the latter, physically accommodate their large size.

On the other hand, there have only been a limited number of enabling technologies using thermal sources 'beyond the THz horizon' (3–30 μm or 10–100 THz) to support wireless communications. This offers opportunities for developing such systems within this largely unregulated part of the electromagnetic spectrum. The '*THz Torch*' concept was recently introduced by the authors for providing secure wireless communications over short distances within the thermal infrared [8–13]. Both single- and multi-channel wireless links have been reported; the resilience to interception and jamming with 2.56 kbps frequency division multiplexing (FDM) and 0.64 kbps frequency-hopping spread-spectrum (FHSS) systems has been demonstrated experimentally [11]. Furthermore, the radiation mechanisms for the basic thermal source transducers [12], as well as the power link budget analysis for the system were previously reported [13]. In this paper, we discuss recent advancements in the front-end enabling technologies associated with the *THz Torch* concept for wireless communications, which go beyond what has already been published.

2 Background

2.1 Single-Channel Wireless Link

The basic architecture for a single-channel thermal infrared *THz Torch* link is deliberately kept simple, as shown in Fig. 1, to keep implementation costs down. With this original setup, the transmitter consisted of five miniature incandescent light bulbs connected in series. The thermally radiated output power was modulated using on-off keying (OOK) with non-return-to-zero (NRZ) pulses and then filtered by an optical coating band-pass filter (BPF).

At the receiver, the input power was first filtered (by an identical optical BPF) and then detected by a pyroelectric infrared (PIR) sensor. The output signal voltage from this detector was further amplified and digitized by the back-end electronics, which contains a baseband low-noise amplifier (LNA), baseband BPF and Schmitt trigger.

The original single-channel *THz Torch* demonstrator [8] operated within an octave 70 % transmittance bandwidth (25–50 THz), which is defined by the optical coating BPF shown in Fig. 2. In practical implementations, PIR detector LME-553, made from lithium tantalate ($LiTaO_3$), was chosen for the following characteristics: (1) detect thermally radiated power, (2) ultra-wide spectral range, (3) room temperature operation capability, (4) relatively fast millisecond response time, and (5) ultra-low cost [16]. The output voltage from the LME-553 was amplified by an LNA having a voltage gain of 100. The signal from the LNA was then filtered by a fourth-order Sallen–Key Butterworth baseband BPF.

Compared to optical wireless communication systems operating at other wavelengths, our thermal-based system is inherently low cost and potentially has a high level of resilience to interference and jamming [11]. With the former, the cost for the complete system is significantly reduced, as thermal sources and detectors have been employed. Systems based on 800-nm LEDs have similar cost and complexity, but LEDs are not spectrally tunable, and the output power has to be limited under a specific safety threshold. In contrast, the output power level and radiance peak for thermal sources can be controlled simply by adjusting the bias current, although this may come with the penalty of lowering spectral power conversion efficiency (from DC). Moreover, our wireless communication system can be considered to be eye-safe, as the shortest operation wavelength is >3 μm. With the latter, it has been experimentally verified that in order to undermine the inherent immunity to interference and interception, both the jammer and intruding receiver, respectively, must be designed to have (1) a significant amount of overlapping spectral channel bandwidths, (2) similar modulation frequency, (3) line-of-sight detection and (4) synchronized hopping pattern (with FHSS) [11]. The main drawbacks of using thermal-based sources are the inherently low switching speed (requiring a separate high-speed modulator) and lack of signal coherency, leaving only the power intensity of the thermal source to be modulated and measured.

2.2 Multi-channel Thermal Infrared *THz Torch* System

With modern communication systems, multiplexing schemes can offer important benefits, including increased overall end-to-end data rates (with band-limited channel assignments) and higher levels of security. Both frequency division multiplexing [10, 11] and frequency-hopping spread-spectrum [11] schemes have been demonstrated with four-channel implementations. To define the four non-overlapping frequency bands, within the thermal infrared, 1-mm-thick

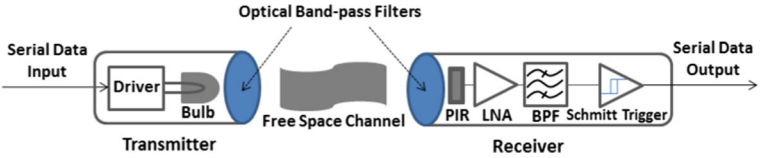

Fig. 1 Basic architecture for single-channel wireless link (modified from [8])

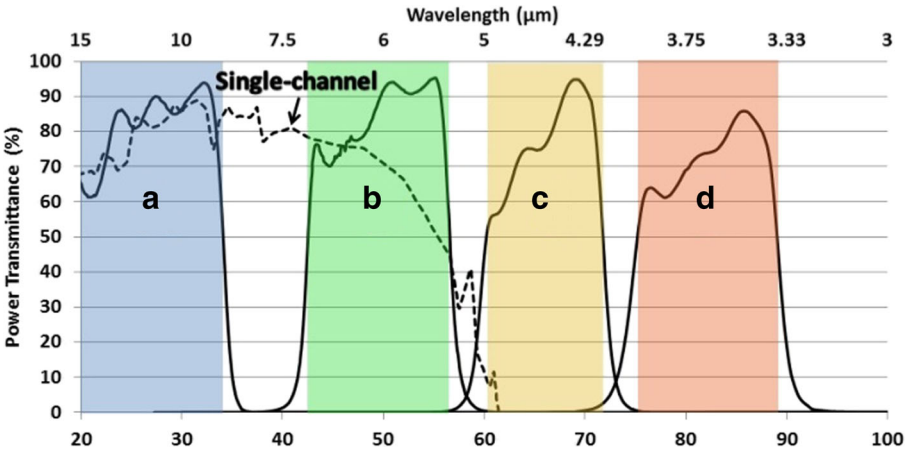

Fig. 2 Measured transmittances for single-channel 70 % transmittance bandwidth filter [14] and multi-channel (*A*, *B*, *C* and *D*) 50 % transmittance bandwidth filters [15]

optical coating band-pass and long-pass filters are used. The measured transmittances for all channel filters are given in Fig. 2, from 20 to 100 THz, for channels A, B, C and D.

The basic architecture for a four-channel *THz Torch* FDM scheme is illustrated in Fig. 3a, where the frequency spectrum is divided up into four non-overlapping frequency bands. Each channel has the same hardware implementation as the single-channel system. In addition to FDM, a FHSS scheme can be implemented to enhance immunity to detection, interception and interference, for secure applications, as illustrated by the proof-of-concept demonstrators shown in Fig. 3b [11]. With the FHSS scheme, the end-to-end serial data stream is transmitted into the same pre-defined channels, but only within one channel at any time—dictated by pseudo-random channel allocation. Slow frequency hopping (SFH) was employed to transmit a 1000-bit data packet through individual channels, within a single hop. For convenience, a pre-determined pseudo-random hopping pattern was applied to both the transmitter and synchronized receiver to establish the secure end-to-end communication link.

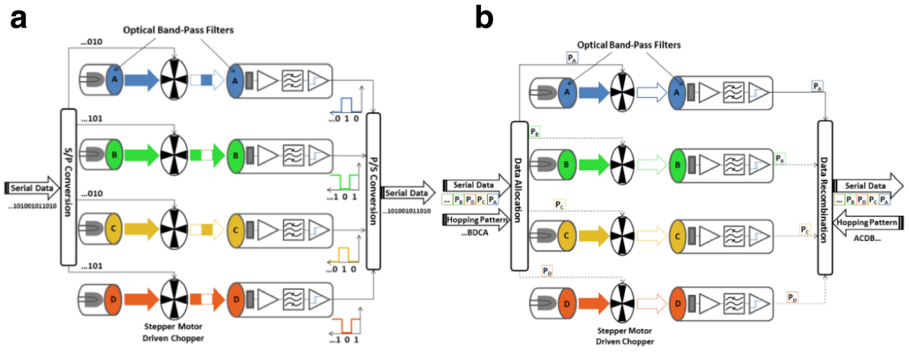

Fig. 3 Proof-of-concept multi-channel *THz Torch* systems. **a** FDM implementation. **b** FHSS implementation (modified from [11])

3 Limitations and Engineering Solutions for *THz Torch* Technology

Until now, the maximum measured data rate reported for current multi-channel thermal infrared *THz Torch* wireless communication systems was 0.64 kbps per channel. This data rate was to a greater extent limited by the rotational speed of the large bespoke (stepper motor-based) mechanical chopper and to a lesser extent by the spectral location and bandwidth of the channel filters [11]. The 25–50 THz (70 % transmittance bandwidth) single-channel system is used to investigate the fundamental performance limitations for the thermal-based wireless link; possible engineering solutions for each limitation are proposed and verified.

3.1 Spreading Loss, Collimating Lenses and Reflectors

Spreading loss has been found to be one of the most significant fundamental limitations, which can be compensated for. Unlike laser sources, which have very narrow beamwidths, radiation from open thermal sources is isotropic. From the Friis equation, in the far field, received power density is inversely proportional to the square of the transmission range [13]. With the previously demonstrated multiplexing systems setup [11], having a range set to 3 cm and bias current of 80 mA (giving a source temperature of 772 K, or total output power of 97.5 mW), the measured bit error rate (BER) was ~10^{-3}.

With thermal sources, the most obvious partial-solution is to introduce a surface aperture, from which energy can be radiated. For example, a high reflectance parabolic surface with cylindrical extension is an efficient solution for maximizing the forward radiated power. A high transmittance collimating lens can then be employed. With the former, reflectors have been widely used in many thermal sources to maximize the output level of radiation from the package. However, to date, no reflector has been used with our experiments. It is believed that future systems will adopt metal-coated parabolic reflectors to enhance the directed power—improving performance significantly.

In principle, potassium bromide (KBr) is an excellent material for making collimating lenses, due to its high transmittance (~90 % transmittance from 0.4 to 20 μm or 15 to 750 THz) and relatively low chromatic dispersion across our spectral range of interest (3 to 30 μm or 10 to 100 THz). Figure 4 shows the power transmittance of KBr with a sample thickness of 10 mm [17].

The 25–50-THz single-channel wireless link was used to evaluate the effectiveness of adopting KBr collimating lenses at both the transmitter and receiver. In this experiment, a standard small (free-running motor-based) optical chopper was employed. Figure 5 shows the

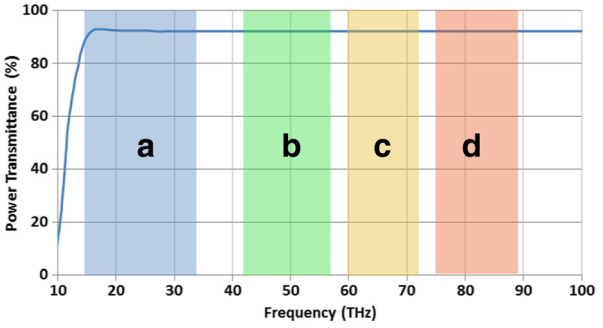

Fig. 4 Power transmittance of 10-mm-thick KBr (raw data sourced from [17])

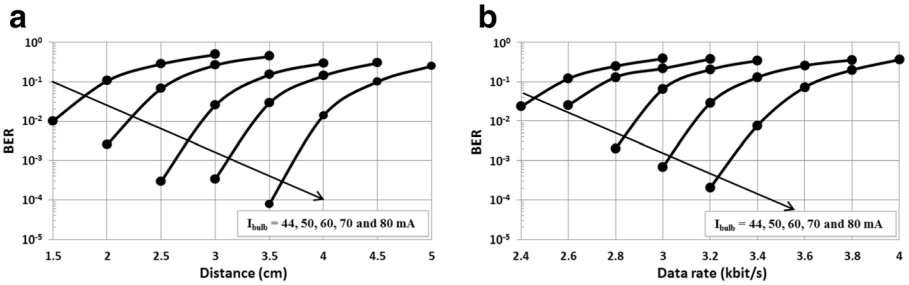

Fig. 5 BER performance for the single-channel *THz Torch* wireless link without lenses: **a** BER against distance with a fixed data rate of 2 kbps; **b** BER against data rate for a fixed range of 1 cm

measured BERs without lenses, as a function of the transmission range and data rate, respectively. Here, the BER was evaluated using 2×10^6 bits of input data. The output voltage from the Schmitt trigger was recorded using a PicoScope 2205 MSO digital oscilloscope and compared with the original binary sequence to record the BER.

The second experiment employs two commercial-off-the-shelf (COTS) 1.5-cm-diameter KBr plano-convex lenses (with a focal length of 1.6 cm). With a fixed distance of 1.6 cm between the lens and the source/sensor, the measured spot size at the receiver is ~2 mm in diameter, which is smaller than the 3.0×3.0 mm^2 sensing element of the detector. Figure 6 shows the new BER performance, as transmission range and data rate are increased from 5 to 17 cm and 2 to 4 kbps, respectively.

As expected, transmission range and BER have improved significantly with the use of lenses. For example, from Figs. 5a and 6a, at 2 kbps and with an 80 mA bias current, range has increased 3.4-fold (from 3.5 to 12 cm); while the BER has also increased 6.2-fold (from 1.3×10^{-5} to 8.0×10^{-5}). Also, from Figs. 5b and 6b, at 3.2 kbps and with an 80-mA bias current, range has increased fivefolds (from 1 to 5 cm); while, the BER has also increased 1.8-fold (from 2.0×10^{-4} to 3.5×10^{-5}). Clearly, with the use of collimating lenses and for the same transmission range, the received power at the detector has increased significantly, resulting in a much better signal to noise ratio. Finally, the measured maximum data rates (with no bit errors for the 2×10^6 bits of input data) against transmission range, with and without KBr collimating lenses, are recorded in Fig. 7. It can be seen that the introduction of lenses dramatically improves both the maximum data rate and transmission range. Moreover, the bit error rate performance is less sensitive to range with the use of lenses.

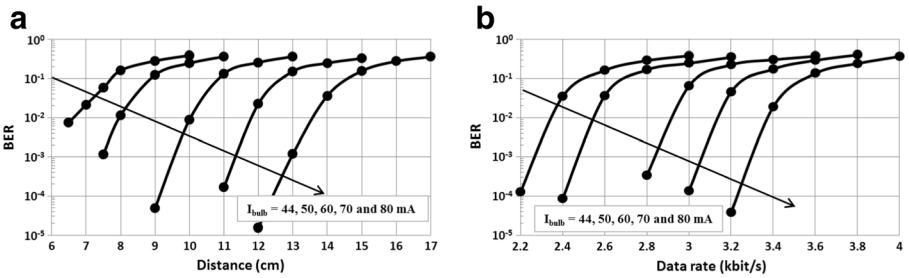

Fig. 6 BER performance for the single-channel *THz Torch* wireless link with two KBr collimating lenses: **a** BER against distance with a fixed data rate of 2 kbps; **b** BER against data rate for a fixed range of 5 cm

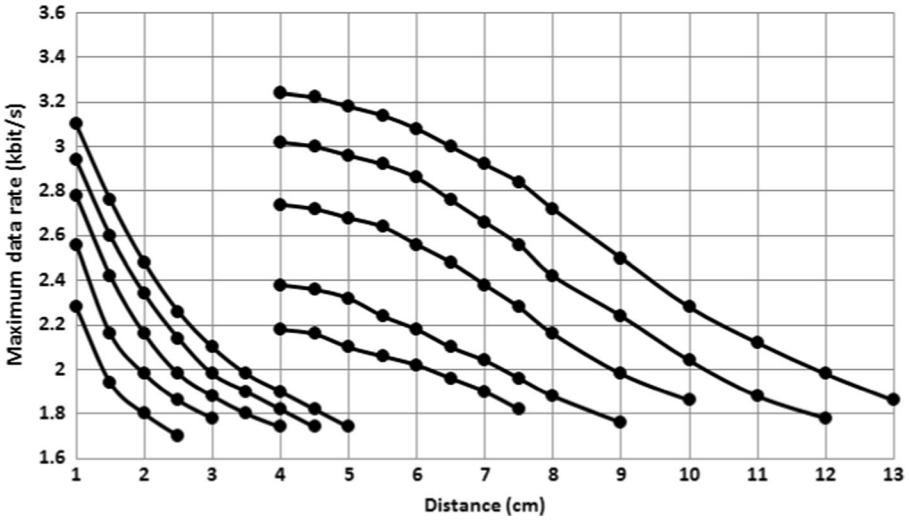

Fig. 7 Maximum data rate for the single-channel '*THz Torch*' wireless link, with and without KBr lenses

3.2 Lens Materials for Thermal Infrared Applications

While having an excellent spectral performance, KBr is hygroscopic and not cost-effective. Materials that exhibit high transmittance and are stable over time are needed. One possibility is to deposit a very thin passivation layer over the KBr lens to provide sufficient hermeticity. Alternatively, non-hygroscopic zinc selenide (ZnSe) also has a high transmittance across a wide spectral range, from 0.5 to 19 μm or 16 to 600 THz. With broadband anti-reflection (BBAR) coatings, ZnSe lenses are commercially available [18]. Moreover, synthetic (CVD-grown) diamond has high transmittance (~70 %) from the far-IR to the ultraviolet range [19]. Another material worth mentioning is the thallium bromoiodide (KRS-5). This material is quite similar to KBr, but much less hygroscopic. Figure 8 shows the power transmittances for these three materials within our spectral range of interest.

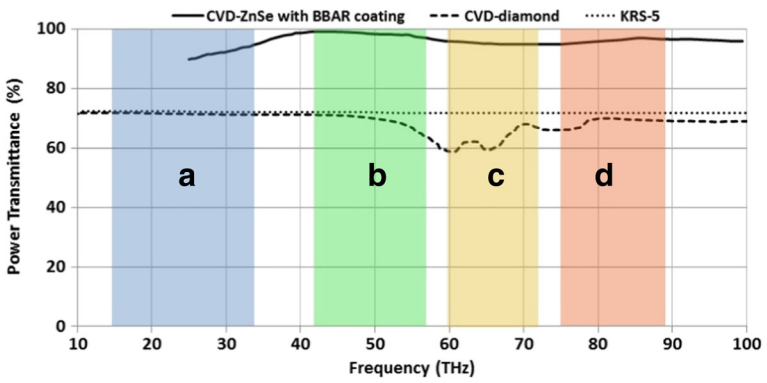

Fig. 8 Power transmittances for 10-mm-thick ZnSe with BBAR coating, 0.5-mm-thick diamond (raw data sourced from [18] and [19], respectively) and 5-mm-thick KRS-5 (raw data sourced from [20])

Polymers also offer transmission windows within the 10 to 100 THz spectral range. For example, polytetrafluoroethylene (PTFE, Teflon) can provide several transmission windows; including 6.7–13.6, 24–33 and 40–300 THz, covering the majority of our spectrum of interest. Polypropylene (PP), high-density polyethylene (HDPE) and polymethylpentene (TPX®) also have transmission windows within the thermal infrared, as shown in Fig. 9. PTFE is particularly noteworthy, as it conforms quite well to our four-channel spectral allocation. Importantly, these polymers are cost-effective and can be fabricated using 3D printing techniques [22, 23], for example, to realize Fresnel lenses with inherently reduced mass, volume and power loss.

3.3 Increased Channel Density

Tungsten filaments are not considered good thermal emitters, due to the large thermal time constant and low emissivity. Moreover, having glass envelopes (e.g. with the miniature COTS incandescent light bulbs used in our earlier proof-of-concept demonstrators), the output radiated power is significantly reduced because of the high absorption of the window glass below ~65 THz [12]. For these reasons, more efficient but also more expensive miniature COTS thermal emitters can be used. When compared to miniature incandescent light bulbs [12], they have higher emissivity (>80 %) elements, similar emitting areas and do not need glass windows [24]. This significantly improves the transmitter's power conversion efficiency. Furthermore, since they can be modulated at higher frequencies (up to 100 Hz), mechanical choppers are no longer needed, making the complete system more compact and lightweight. In addition, real (or pseudo-random binary sequence) data can be transmitted at relatively much higher rates since inertia limitations associated with stepper motor-based mechanical choppers are avoided.

Moreover, with the considerably more thermally radiated output power available from COTS thermal emitters, with sizes comparable to incandescent light bulbs, the channel bandwidth can be reduced to maintain the minimum required output power to meet operational needs. As a result, more channels can be introduced within the same spectral range of interest.

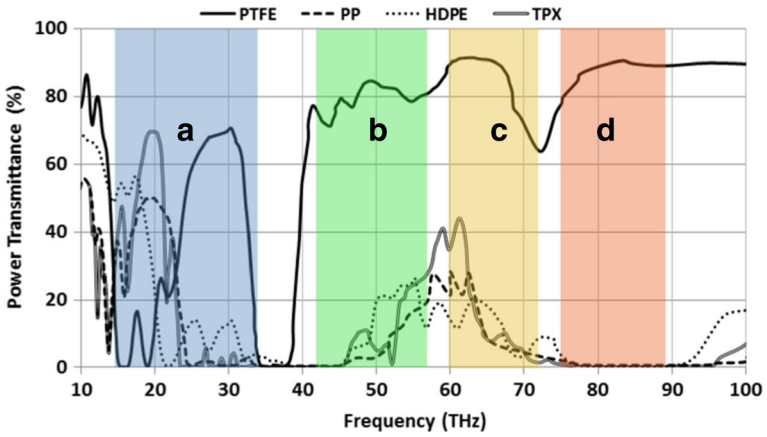

Fig. 9 Power transmittance for various IR transparent polymers having thicknesses of 1 mm for PTFE and 2 mm for PP, HDPE and TPX (raw data sourced from [21])

Without the mechanical chopper, each channel operates at the lower speed of 100 Hz but can still maintain or increase the end-to-end data rate.

For example, if an end-to-end data rate of 4 kbps is required, a four-channel system has to operate at 1 kbps per channel. This channel data rate cannot be achieved easily by the thermal emitter alone (as it may require an additional external modulator) and is not optimal for most pyroelectric sensors. With the former, COTS thermal emitters normally have a rise/fall time of ~10 ms, giving a typical highest modulation frequency of 100 Hz [24]. Some vacuum emitters can have a rise/fall time of ~5 ms, further increasing the modulation frequency [25]. With the latter, the LME-553 detector has a flat detectivity spectral response between 10 and 60 Hz, as shown in Fig. 10a. With a 1-kHz modulation speed, the signal to noise ratio (SNR) of the complete system is degraded, due to having a lower specific detectivity relative to the optimal modulation region of 10 to 60 Hz. Having said this, the LME-553 detector can still operate up to several kilohertz, as long as the minimum required input power meets operational needs. By introducing 16 channels, each operates at 250 Hz, closer to the optimal operation range, which further improves the SNR performance.

Sixteen-channel thermal infrared *THz Torch* systems are currently being developed for a variety of different applications. For example, with coarse spectroscopy, 16 matched pairs of COTS narrowband BPFs, within the spectral range from 20 to 80 THz, provide 16 discrete spectral data points. As can be seen from Fig. 10b, the filter specifications and spectral coverage are not ideal, due to the inherent limitations of optical coating filters. However, it was still possible to sample the spectral range of interest. The measured power ratio (power transmittance in transmission mode or reflectance in reflection mode) with and without a sample under test can be compared with pre-characterized spectral signatures with a material database. The resulting spectrometer can operate at room temperature, be lightweight, compact and at a very low cost [26, 27]. Unfortunately, optical coating filters are not frequency-scalable, which limits filter specifications and spectral coverage availability.

3.4 Integrated Frequency-Selective Thermal Emitters

In principle, the thermally radiated output power from a blackbody source can be spectrally filtered by an inductive (band-pass) metal mesh filter [28]. However, at thermal infrared frequencies, free-standing metal mesh filters are not mechanically robust, as the thickness of the metal layer has to be kept thin in order to avoid waveguide

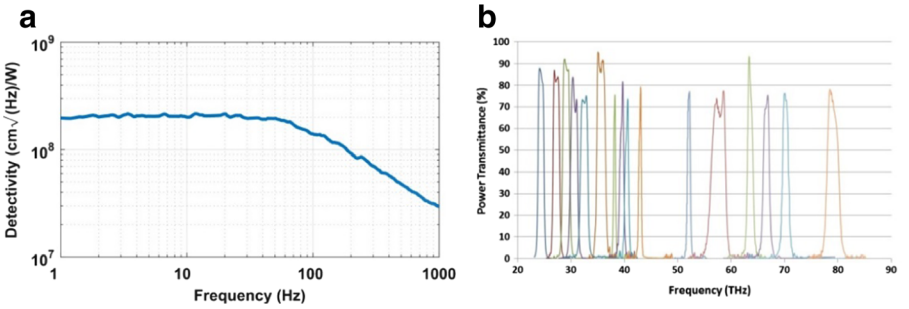

Fig. 10 **a** Measured detectivity versus modulation frequency for the LME-553 sensor [16] and **b** power transmittances for the 16-channel narrowband filters

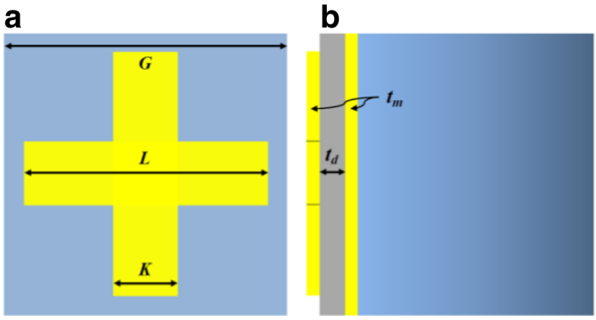

Fig. 11 Layout of a frequency-selective thermal emitter operating at 50 THz. **a** Top view and **b** side view

modes, while substrate-based filters will have a Fabry–Pérot etalon, since the thickness of substrate is comparable to the wavelength inside. Therefore, at thermal infrared frequencies, both types of filters face challenges in terms of design and fabrication.

As an alternative to using wideband thermal emitters (such as blackbody sources), frequency-selective thermal emitters can be employed, having a dielectric spacer layer that is thin enough to avoid in-band Fabry–Pérot resonances. According to Kirchhoff's law of thermal radiation, the absorptance of a material at thermal equilibrium is equal to its emissivity. Therefore, high absorptance (emissivity) can be obtained from a structure that minimizes both transmittance and reflectance. Cross-shaped capacitive metal mesh structures have been used to create near-blackbody radiators/absorbers with frequency-selective properties within the terahertz [29], mid-infrared [30], offering the ability to engineer the desired spectral emissivity profile within the thermal infrared.

For example, with the frequency-selective thermal emitter design shown in Fig. 11, CST Microwave Studio® was used to perform numerical simulations (in both time and frequency domains) with dimensional parameter sweeps to achieve a centre frequency of 6 μm or 50 THz. The top cross-shaped resonator is made from a thin gold layer (with thickness $t_m = 100$ nm). The lattice constant $G = 2.2$ μm, cross-length $L = 1.9$ μm and cross-width $K = 0.5$ μm. An Al_2O_3 dielectric spacer layer (with thickness $t_d = 200$ nm) is introduced between the two metal layers. Since the bottom screening metal layer is thicker than the skin depth of gold at the lowest frequency of interest, there will be zero transmittance [31]. Finally, a rigid substrate is used for structural support (its dielectric properties are not important), as well as serving as a heat sink (if used as an emitter).

For angular frequency ω, transmittance $T(\omega) = |S_{21}(\omega)|^2$ and reflectance $R(\omega) = |S_{11}(\omega)|^2$ are obtained from simulated scattering (S-) parameters, and the absorptance $A(\omega)$ is then calculated as $A(\omega) = 1 - T(\omega) - R(\omega)$. Figure 12 shows the resonance frequency $f_r = 50$ THz, corresponding absorptance $A = 95.9$ % and fractional bandwidth $BW = 19.6$ %.

To use frequency-selective thermal emitters for *THz Torch* applications, the frequency-size scalability of the design needs to be evaluated over the spectral range of interest. The scaling factor is defined as the ratio of the new to the 50-THz reference resonance frequencies. By linear scaling all the dimensional parameters shown in Fig. 11, the predicted simulated resonance frequency, corresponding absorptance peak and fractional bandwidth are shown in Fig. 13. It can be seen that frequency-size scalability is near-linear over the entire spectral range of interest.

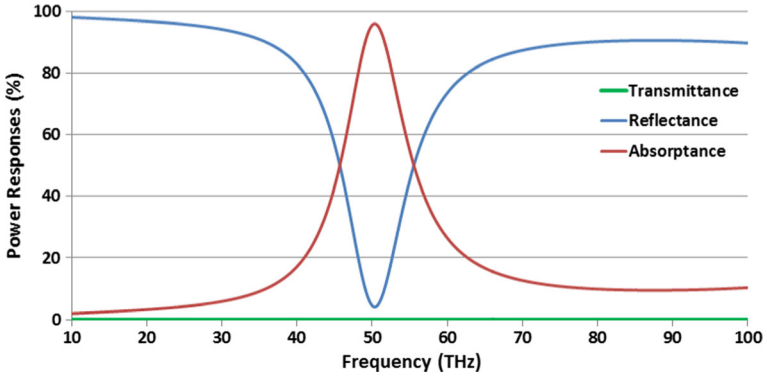

Fig. 12 Simulated transmittance, reflectance and absorptance for a frequency-selective thermal emitter

A scaling error can be associated with each performance parameter using

$$e_s = \frac{P_{\text{simulated}} - P_{\text{predicted}}}{P_{\text{predicted}}} \cdot 100\%$$

where $P_{\text{simulated}}$ and $P_{\text{predicted}}$ represent the simulated and predicted values of the performance parameter (e.g. resonance frequency), respectively. It has been found that the absorptance peak shows the best linear scalability (with $|e_s| < 2\,\%$), followed by the resonance frequency (with $|e_s| < 5\,\%$). Although the fractional bandwidth is not linearly scalable (with $|e_s| \sim 25\,\%$), this parameter is of lesser importance and can be further optimized as necessary.

One of the advantages of using frequency-selective thermal emitters is that each channel source can have a be-spoke design, in terms of resonance frequency, emissivity and fractional bandwidth. This removes the need for commercial emitters and optical coating filters. Moreover, the design and implementation of frequency-selective emitters can be arrayed onto a single substrate, leading to an integrated module that is lightweight, compact and low cost. One of the challenges for these frequency-selective thermal emitters is that in order to obtain a high output power, the temperature of the emitter has to be increased (e.g. to ~500 K), and the material deformation and degradation have to be considered.

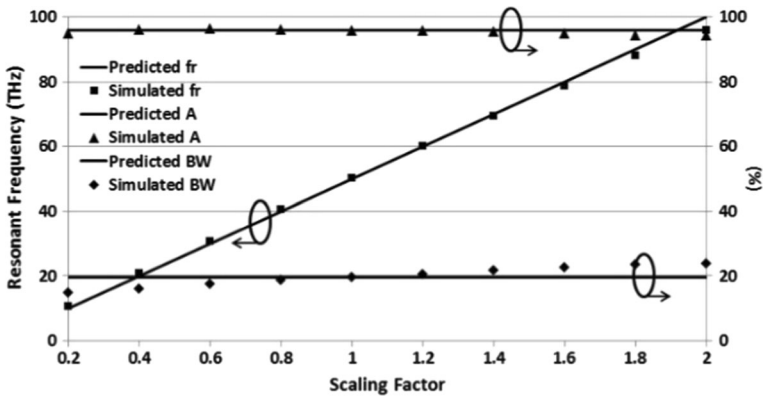

Fig. 13 Scalability for the frequency-selective thermal emitter in Fig. 11

4 Conclusions

In this paper, we first briefly introduced the *THz Torch* technology, along with its hardware requirements. Fundamental limitations associated with the front-end hardware were identified; engineering solutions are then proposed and verified. For example, free-space spreading loss can be compensated for by employing reflectors (e.g. Winston cone) and collimating lenses made from suitable materials. Moreover, channel density can be increased by using commercially available thermal sources or be-spoke frequency-selective emitters.

New simulation/experimental results are given to quantify the effects of introducing engineering improvements in a number of enabling front-end technologies (not previously demonstrated with our specific *THz Torch* application); while comparing and contrasting other technologies act as a useful review. Collectively, we believe that our paper points to a raft of engineering solutions that will significantly improve the performance of future systems and thus further promote the new application.

These practical engineering solutions are expected to be implemented in next-generation wireless communication systems; improving both the data rate and transmission range. Moreover, with the continual advancements being made in front-end thermodynamics, back-end electronics and signal processing, other *THz Torch* applications are beginning to emerge, such as spectroscopy [26, 27] and imaging (with 2D scanners and 3D tomography). With these applications, purely reflective optics can be used in the experimental setups, which are low loss, more broadband and cheaper than having IR lenses.

Acknowledgments This work was in part supported by the China Scholarship Council (CSC). The authors would like to thank Dr Mark Bailey at Northumbria Optical Coatings Ltd. for the kind donation of the 16 pairs of narrow band-pass filters and associated measured data.

References

1. S. Bloom, E. Korevaar, J. Schuster and H. Willebrand, "Understanding the performance of free-space optics", *Journal of Optical Networking*, vol. 2, no. 6, 178–200 (2003)
2. J. M. Kahn and J. R. Barry, "Wireless infrared communications", *Proceedings of the IEEE*, vol. 9219, no. 97, 265–298 (1997)
3. M. Achour, Free-space optics wavelength selection: 10 μm versus shorter wavelengths, *Journal of Optical Networking*, vol. 2, no. 6, 127–143 (2003)
4. E. Leitgeb, T. Plank, M. S. Awan, P. Brandl, W. Popoola, Zabih Ghassemlooy, F. Ozek and M. Wittig, "Analysis and evaluation of optimum wavelengths for free-space optical transceivers", in *IEEE 12th International Conference on Transparent Optical Networks (ICTON)*, 1–7 (2010)
5. Y. Yao, A. J. Hoffman and C. F. Gmachl, Mid-infrared quantum cascade lasers, *Nature Photonics*, vol. 6, 432–439 (2012)
6. S. Blaser, D. Hofstetter, M. Beck and J. Faist, Free-space optical data link using Peltier-cooled quantum cascade laser, *Electronics Letters*, vol. 37, no. 12, 778–780 (2001)
7. A. Pavelchek, R. G. Trissel, J. Plante and S. Umbrasas, "Long-wave infrared (10-micron) free-space optical communication system", in *Proc. SPIE 5160, Free-Space Laser Communication and Active Laser Illumination III*, doi: 10.1117/12.5049406 (2004)
8. S. Lucyszyn, H. Lu and F. Hu, "Ultra-low cost THz short-range wireless link", in *IEEE International Microwave Workshop Series on Millimeter Wave Integrated Technologies*, Sitges, Spain, 49–52 (2011)

9. F. Hu, X. Liang and S. Lucyszyn, "Multi-channel thermal infrared communications using engineered blackbody radiation for security applications", in *SPIE Security + Defence 2014*, Amsterdam, The Netherlands (2014)
10. F. Hu and S. Lucyszyn, "Emerging thermal infrared '*THz Torch*' technology for low-cost security and defence applications", Chapter 13, in "*THz and Security Applications: Detectors, Sources and Associated Electronics for THz Applications*", NATO Science for Peace and Security Series B: Physics and Biophysics, ed. By C. Corsi and F. Sizov (Springer Netherlands, 2014), 239–275
11. X. Liang, F. Hu, Y. Yan and S. Lucyszyn, "Secure thermal infrared communications using engineered blackbody radiation", *Scientific Reports*, *Nature Publishing Group*, vol. 4 (2014)
12. F. Hu and S. Lucyszyn, Modelling miniature incandescent light bulbs for thermal infrared 'THz Torch' applications, *Journal of Infrared, Millimeter, and Terahertz Waves*, vol. 36, no. 4, 350–367 (2015)
13. F. Hu, J. Sun, E. H. Brindley, X. Liang and S. Lucyszyn, Systems analysis for thermal infrared 'THz Torch' applications, *Journal of Infrared, Millimeter, and Terahertz Waves*, vol. 36, no. 5, 474–495 (2015)
14. Murata Manufacturing Co., Ltd., "Pyroelectric infrared sensors", 2012. [Online]. Available: http://www.murata.com/media/webrenewal/support/library/catalog/products/sensor/infrared/s21j.pdf
15. Northumbria Optical Coatings Ltd., "Online catalogue for optical coating bandpass filters", 2011, [Online]. Available: http://www.noc-ltd.com/catalogue
16. InfraTec "LME-553 datasheet", 2012. [Online]. Available: http://www.infratec-infrared.com/Data/LME-553.pdf
17. Global Optics UK Ltd., "Potassium Bromide—KBr", 2012, [Online]. Available: http://www.globalopticsuk.com/potassium-bromide.htm.
18. Tydex®, "Online catalogue: CVD-ZnSe for pyrometry", 2014, [Online]. Available: http://www.tydexoptics.com/pdf/ZnSe_for_pyrometry.pdf
19. Diamond Materials, "CVD diamond booklet", 2014, [Online]. Available: http://www.diamond-materials.com/downloads/cvd_diamond_booklet.pdf
20. ISP Optics Corp., "Thallium Bromoiodide (TlBr–TlI) datasheet", 2013, [Online]. Available: http://www.ispoptics.com/admuploads/file/krs_5.pdf
21. Tydex®, "Online catalogue: THz materials", 2014, [Online]. Available: http://www.tydexoptics.com/pdf/THz_Materials.pdf
22. S. F. Busch, M. Weidenbach, M. Fey, F. Schäfer, T. Probst and M. Koch, Optical properties of 3D printable plastics in the THz regime and their application for 3D printed THz optics, *Journal of Infrared, Millimeter, and Terahertz Waves*, vol. 35, no. 12, 993–997 (2014)
23. LUXeXceL, "3D printed optics", 2015. [Online]. Available: http://www.luxexcel.com/
24. Electro Optical Components Inc., "Online catalogue", 2014, [Online]. Available: http://www.eoc-inc.com/infrared_source.htm
25. D. A. Saylor, D. B. Beasley, B. Braselton and J. A. Buford, Jr. "Current status of IR scene projection at the U.S. Army Aviation and Missile Command", Proc. SPIE 4366, Technologies for Synthetic Environments: Hardware-in-the-Loop Testing VI (2001). [Online]. Available: http://dx.doi.org/10.1117/12.438066
26. J. Sun, F. Hu and S. Lucyszyn, "Challenges for the development of low cost thermal infrared 'THz Torch' spectrometers", in *4th Annual Conference AnalytiX-2015*, Nanjing, China (2015) (Invited)
27. J. Sun, F. Hu, Z. Wang and S. Lucyszyn, "Banknote characterization using a thermal infrared 'THz Torch' spectrometer, *Asia-Pacific Microwave Conference (APMC2015)*, Nanjing, China (2015) (Invited)
28. W. J. Otter, F. Hu, J. Hazell and S. Lucyszyn, "THz metal mesh filters on electrically thick fused silica substrates", *39th International Conference on Infrared, Millimeter, and Terahertz Waves (IRMMW-THz)*, Tucson, USA (2014)
29. F. Hu, W. J. Otter and S. Lucyszyn, "Optically tunable THz frequency metamaterial absorber", *40th International Conference on Infrared, Millimeter, and Terahertz Waves (IRMMW-THz)*, Hong Kong, China (2015)
30. X. Liu, T. Tyler, T. Starr, A. F. Starr, N. M. Jokerst and W. J. Padilla, Taming the blackbody with infrared metamaterials as selective thermal emitters, *Physical Review Letters*, vol. 107, 045901–1 (2011)
31. S. Lucyszyn and Y. Zhou, Characterising room temperature THz metal shielding using the engineering approach, *PIER Journal*, vol. 103, pp. 17–31, 2010